Cardiovascular Engineering and Technology, Vol. 10, No. 1, March 2019 *(© 2018)* pp. 173–180
https://doi.org/10.1007/s13239-018-00375-1

Quantitative Characterization of Aortic Valve Endothelial Cell Viability and Morphology *In Situ* Under Cyclic Stretch

SCOTT A. METZLER,[1] STEVEN C. WALLER,[1] and JAMES N. WARNOCK[1,2]

[1]Department of Agricultural and Biological Engineering, Mississippi State University, Mississippi State, MS 39762, USA; and [2]School of Chemical, Materials & Biomedical Engineering, University of Georgia, 220 Riverbend Road, Athens, GA 30602, USA

(Received 11 June 2018; accepted 17 August 2018; published online 23 August 2018)

Associate Editor Hanjoong Jo oversaw the review of this article.

Abstract—Current protocols for mechanical preconditioning of tissue engineered heart valves have focused on application of pressure, flexure and fluid flow to stimulate collagen production, ECM remodeling and improving mechanical performance. The aim of this study was to determine if mechanical preconditioning with cyclic stretch could promote an intact endothelium that resembled the viability and morphology of a native valve. Confocal laser scanning microscopy was used to image endothelial cells on aortic valve strips subjected to static incubation or physiological strain regimens. An automated image analysis program was designed and implemented to detect and analyze live and dead cells in images captured of a live aortic valve endothelium. The images were preprocessed, segmented, and quantitatively analyzed for live/dead cell ratio, minimum neighbor distance and circularity. Significant differences in live/dead cellular ratio and the minimum distance between cells were observed between static and strained endothelia, indicating that cyclic strain is an important stimulus for maintaining a healthy endothelium. In conclusion, *in vitro* application of physiological levels of cyclic strain to tissue engineered heart valves seeded with autologous endothelial cells would be advantageous.

Keywords—Image analysis, Endothelium morphology, Aortic valve, Tissue engineering.

INTRODUCTION

Heart valve disease affects 2.5% of the US population and approximately 10% of the population ≥ 65 years old.[2] Two thirds of valve disorders occur in the aortic position with ≈ 50% resulting in Total Aortic Valve Replacement (TAVR) surgery.[1] These numbers are expected to increase over the coming decades and simulations project the global incidence of aortic stenosis could double or even triple in the next 30–40 years.[8,21] Aortic valve calcification is the primary indication for TAVR surgery in Europe and the United States[6] and is the second most common cardiovascular surgery performed.[29] The current options for valve replacement include mechanical valves, xenogenic bioprosthetic valves or biological valves such as homografts.[31] Mechanical valves require patients to be on continuous anti-coagulation therapy to prevent the formation of thrombi, making them unsuitable for elderly patients.[9,13] Bioprosthetic valves do not require patients to be on anti-coagulation therapy; however, as they are xenogenic, they must be treated with aldehyde-based fixatives to prevent an immunological host response. Chemical fixation makes valves susceptible to inflammation, calcification and deterioration *via* mechanical fatigue[18] or incomplete fixative detoxification.[11,26] Therefore, there is a critical need for a tissue engineered heart valve that has excellent hemodynamics, a capacity for tissue remodeling and an ability to grow with the patient.

Tissue engineered heart valves (TEHV) are comprised of a porous scaffold, usually made from biodegradable synthetic polymers or decellularized tissue,[3] and a cell population that mimics the native population of valve interstitial cells (VIC) and endothelial cells (EC). A number of cell sources have been investigated for TEHVs, including stem cells, VICs, ECs, myofibroblasts, endothelial progenitor cells, and smooth muscle cells.[28] A number of studies have demonstrated that mechanical pre-conditioning of the seeded scaffold is necessary before implantation. For a comprehensive review of TEHV recellularization and pre-conditioning, see the review by VeDepo *et al.*[31] Studies have largely focused on the application of pressure and/or flow. Research on native valve tissue

Address correspondence to James N. Warnock, School of Chemical, Materials & Biomedical Engineering, University of Georgia, 220 Riverbend Road, Athens, GA 30602, USA. Electronic mail: james.warnock@uga.edu

has shown that physiological mechanical conditions maintain the biological characteristics of aortic heart valves[14] and the application of pressure can stimulate collagen and glycosaminoglycan synthesis.[20,34,35] To date, few studies have investigated the advantages of using cyclic strain for the mechanical pre-conditioning of TEHV. Cyclic strain has been shown to protect valves from pro-inflammation gene and protein expression[17,27] and it could also provide other benefits in TEHV pre-conditioning.

The purpose of this study was to determine how cyclic strain affects aortic valve EC morphology, viability and confluence. A cyclic strain device was developed to exert physiological strain on aortic valve tissue and a custom MatLab code was written to perform quantitative analysis of live *en face* microscopy images of leaflet surfaces. Results from the study will improve our understanding of the relationship between aortic valve ECs and their mechanical environment as well as provide information applicable to the development of TEHV using mechanical preconditioning techniques.

METHODS

Tissue Preparation

Porcine hearts were obtained from female Yorkshire/Hampshire pigs before 6 months of age with a post-slaughter weight of 120 lbs. Aortic valve leaflets were excised within 30 min of slaughter (Sansing Meat Service, Maben, MS) and transported to the lab in sterile phosphate buffered saline (D-PBS, Sigma) on ice. The leaflets were excised aseptically with a razor blade as previously described.[33] Care was taken to not disrupt the endothelial layer. Leaflet strips were randomly separated into three treatment groups: fresh, static, and stretched. Fresh tissue samples were stained immediately as described below. Static samples were placed in a six-well plate and incubated with 3 mL of culture medium (Dulbecco's modified eagles medium (DMEM, Sigma) supplemented with 10% fetal bovine serum (FBS, Atlanta Biological)) and incubated at 37 °C in 5% CO_2 for 72 h. Stretched samples were attached to a custom uniaxial cyclic stretcher filled with culture medium and underwent 15% cyclic stretch at 1 Hz for 72 h. The stretch device was placed in an incubator to maintain temperature at 37 °C. Following stretching or static incubation, samples were stained and imaged identically to fresh samples.

Live Cell En face Imaging

The ventricularis and fibrosa endothelia were imaged *en face* as previously described.[16] Briefly, leaflets were stained with calcein-AM (5 μM), ethidium homodimer (5 μM) and Hoechst 33342 (1 μM, Invitrogen) for 15 min. Leaflet strips were rinsed twice in PBS and placed on a 1 mm thick glass slide. A 22 × 22 mm 1 oz glass coverslip was gently placed on the tissue and held on by capillary action. The coverslip aided in providing a more planar cellular surface where a large enough region of interest could be analyzed while maintaining a relatively uniform focal plane. The Zeiss LSM 510 confocal microscope was used in the plane-scanning mode to acquire each image at a single focal z-plane. 3D image stacks were not created due to the additional processing required. The objective used was an EC Plan-Neofluar 10X, with a numerical aperture (NA) of 0.30. Beam splitters split the laser lines at 405, 488, and 543 nm for the red, green, and blue channels, respectively. Filters for fluorescent detection were a band pass 420–480 (blue), band pass 505–530 (green) and a long pass 615 for the red channel.

Image Analysis

The preprocessing step was composed of background subtraction, channel image subtraction, and transformation to a binary image. Background subtraction involved first constructing the background image using block processing and subtracting the result from the channel image. Channel image subtraction was performed to subtract nuclei information from each channel image. Due to the fact that nuclei are present in all cells, and the fluorescent stain is highly permeable, precise determination of the origin of nuclei fluorescence was unattainable. Therefore, the nuclei components were subtracted and ignored for live and dead cell statistical analysis. Channel image subtraction was carried out by subtracting the blue channel, including nuclei information, from the red or green channel image using Eq. (1).

$$I_{\text{channel}} = I_{\text{channel}} - \lambda \cdot I_{\text{blue}}, \tag{1}$$

where I is the weighting factor, $0 < \lambda \leq 1$, depending on the channel. A thresholding technique was used to change the image into a binary image. To determine the individual thresholds, Otsu's method was employed.[22] Figure 1 shows the sequence of image processing for live cells (Figs. 1a, 1b, 1c, and 1d) and predominantly dead cells (Figs. 1e, 1f, 1g, and 1h).

Information was extracted from processed images using a custom Matlab program. Number of live cells, dead cells, area, perimeter, circularity, aspect ratio, orientation, and the minimum neighbor distance were calculated. This information was used to calculate live/dead cell ratio, which is defined in Eq. (2).

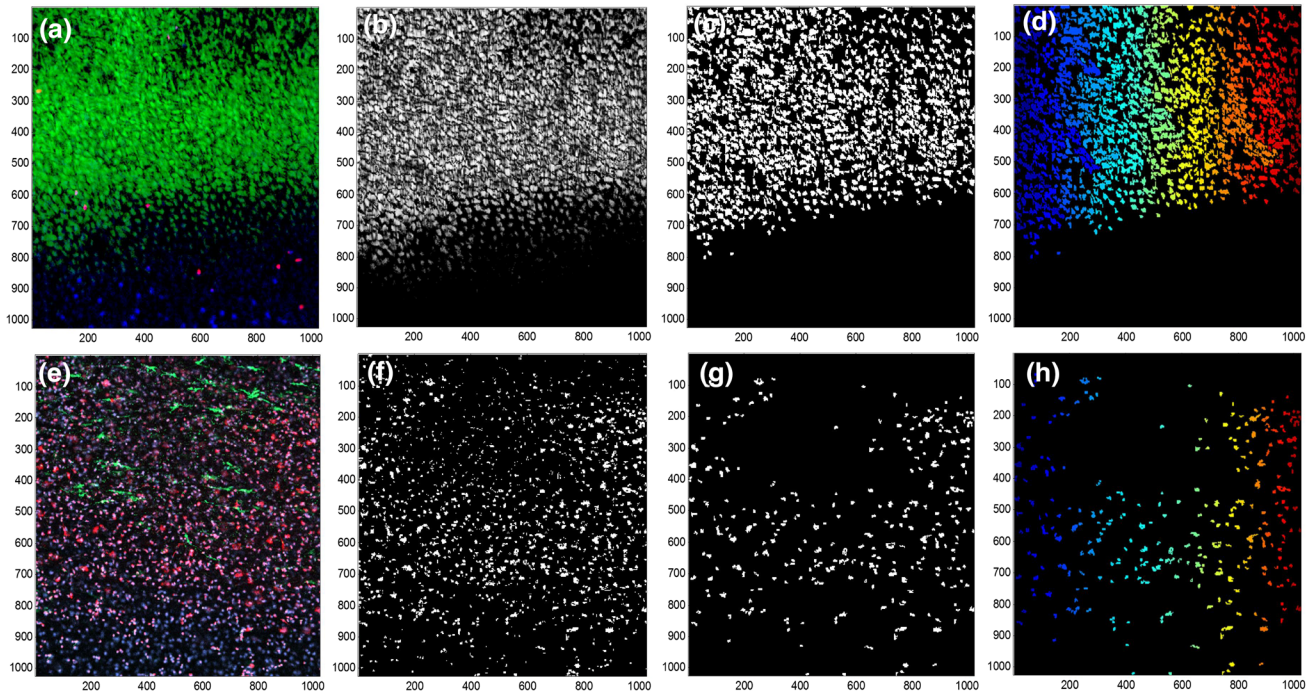

FIGURE 1. Image post-processing using custom code for Digital Image Processing Toolbox in Matlab. A representative particle analysis workflow is shown for live (a–d) and dead (e–h) cells. Raw images (a, e) are thresholded using Otsu's method (b, f), segmented (c, g), and labeled (d, h) for morphological analysis.

$$\text{Cell Ratio} = \frac{X_v}{X_v + X_d}, \tag{2}$$

where X_v is the number of viable cells and X_d is the number of dead cells. Cell circularity was measured using Eq. (3).

$$\text{Circularity} = \frac{4\pi \cdot \text{Area}}{\text{Perimeter}^2} \tag{3}$$

Stretched tissue was compared with fresh tissue (i.e., immediately following slaughter) and tissue incubated under static conditions for the same duration as the stretch experiments.

Statistical Analysis

Four images were taken for each sample condition. Results for aspect ratio, circularity and minimum neighbor distance are reported as mean ± 95% confidence interval. One-way analysis of variance (ANOVA) was performed using SAS analysis software to determine significant differences (p value ≤ 0.05).

RESULTS

Cell Viability

En face imaging of the aortic valve surface was performed using confocal laser scanning microscopy. Figures 2a and 2d show fresh leaflets exhibited a nearly confluent endothelium, as seen by the presence of green cells and comparably few red cells. There were no distinct differences between the fibrosa and ventricularis layers. Static control leaflets showed that, in the absence of mechanical stimulation, the aortic valve endothelium experienced significant cell death (see Figs. 2b and 2e). There was a clear loss of live green cells, while the number of dead cells increased drastically when compared to the fresh leaflet strips. Aortic valve leaflets that were cyclically stretched displayed a highly side-dependent endothelium strain response (see Figs. 2c and 2f). Leaflets showed a near confluent endothelium on the fibrosa; however, leaflets showed a decrease in live cells on the ventricularis.

Quantification of the endothelium confirmed the qualitative observations. Figure 3a shows the total cell count obtained collectively from the four independent leaflet samples. These values were used to calculate the percentage of live cells in each of the sample groups. As seen in Fig. 3b, fresh leaflet tissue had 98 and 97% viable cells on the fibrosa and ventricularis, respectively. The percentage of viable cells decreased significantly after 72 h of static incubation, with 34 and 22% viability on the fibrosa and ventricularis, respectively. Cyclic stretch was able to maintain viability over 72 h, especially in the fibrosa where the percentage of live cells was calculated as 96%. Endothelial cell viability on the ventricularis was reduced to 68%, which was

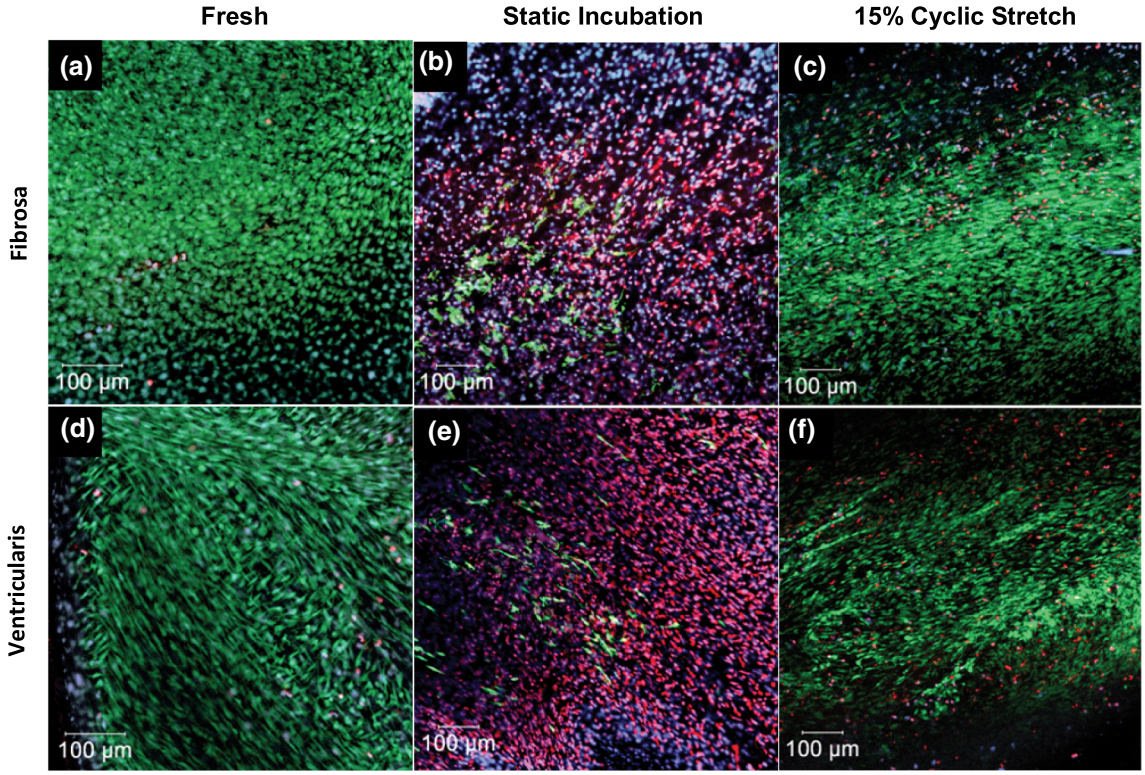

FIGURE 2. Representative images of porcine aortic valve leaflet strips from fresh tissue (a, d) tissue incubated under static conditions for 72 h (b, e) and tissue incubated with cyclic stretch for 72 h (c, f). Live EC staining positive for Calcein-AM are seen in green on the fibrosa (a–c) and ventricularis (d–f), while dead EC staining positively for Eth-1D are visualized in red, as well as nuclei seen in blue depicting fluorescent Hoechst 33342.

significantly lower than the fibrosa but was three times greater than viability in static cultures.

Cell Morphology

Morphology of viable cells was assessed by measuring the circularity, as shown in Fig. 4. The circularity of endothelial cells on the fibrosa in fresh tissue samples was calculated as 0.58. When incubated under static conditions for 72 h, circularity decreased to 0.54. When stretched for 72 h, circularity was decreased further to 0.48. Endothelial cells on the ventricularis of fresh tissue had a circularity of 0.48. This increased to 0.50 under static conditions but statistical analysis showed that this increase was not statistically significant. When cells were exposed to cyclic stretch, the circularity of endothelial cells on the ventricularis decreased to 0.465, which was considered statistically significant compared to static tissue but not when compared to fresh tissue.

The circularity of endothelial cells on the fibrosa was statistically significantly higher on the fibrosa than the ventricularis in fresh tissue and statically incubated tissue. However, when tissue was stretched for 72 h, there was no significant difference in circularity between cells on either side of the tissue (Fig. 4).

Cell Confluence

Confluence was determined by measuring the minimum neighbor distance (MND), with lower values between viable cells indicating greater confluency. Fresh tissue had an MND of 6.39 ± 0.184 μm on the fibrosa and 6.42 ± 0.176 μm on the ventricularis. Following static incubation, confluency decreased as MND increased to 12.61 ± 0.851 μm on the fibrosa and 13.97 ± 1.117 μm on the ventricularis. Tissue exposed to cyclic stretch also saw a decrease in cell confluency but to a lesser extent compared to statically incubated tissue. The MND for stretched tissue was 7.55 ± 0.276 μm on the fibrosa and 7.27 ± 0.323 μm on the ventricularis. Under each condition, there was no significant difference in the MND between the fibrosa and ventricularis as shown in Fig. 5.

DISCUSSION

During the cardiac cycle, the aortic valve endothelium experiences anisotropic biaxial strain. Strain is the result of the pressure difference between the aorta and left ventricle, which during diastole is 80 mmHg. The tensile strain has been estimated to be 11% in the

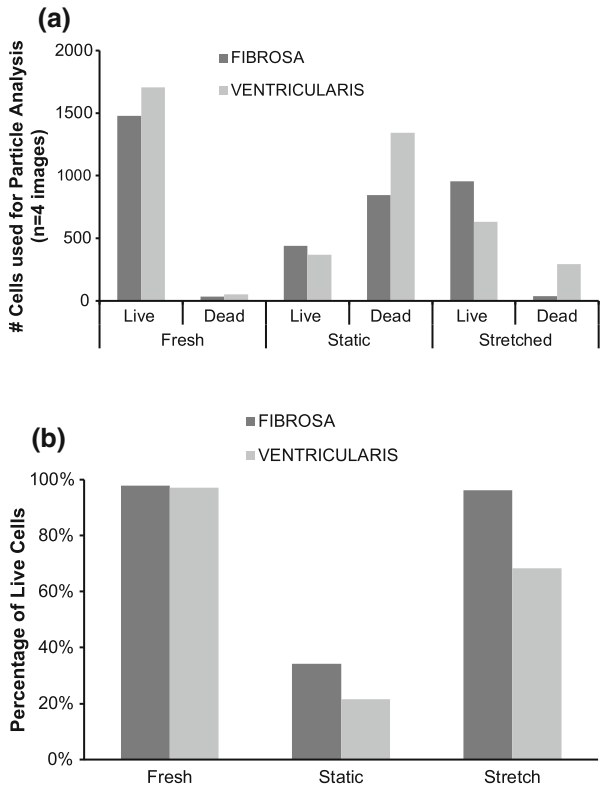

FIGURE 3. Total number of cells captured from four tissue samples and used for analysis (a) and the ratio of live cells to total cells (b) under each condition.

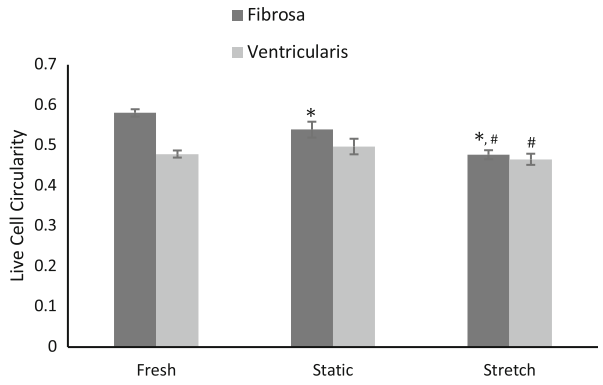

FIGURE 4. Live cell circularity of cells on the fibrosa and ventricularis surfaces of aortic heart valves. * denotes a significant difference with fresh leaflet samples, # denotes significant difference with static leaflet samples, $p < 0.05$. Error bars represent 95% confidence interval.

circumferential direction and 13–25% in the radial direction.[36] The current study showed that application of cyclic strain at normal physiological levels was able to maintain endothelium viability at levels similar to fresh valve tissue, whereas static conditions caused a significant reduction in EC viability. These data are consistent with previous studies that used real-time, live *en face* imaging of aortic valve leaflets in an *ex vivo*

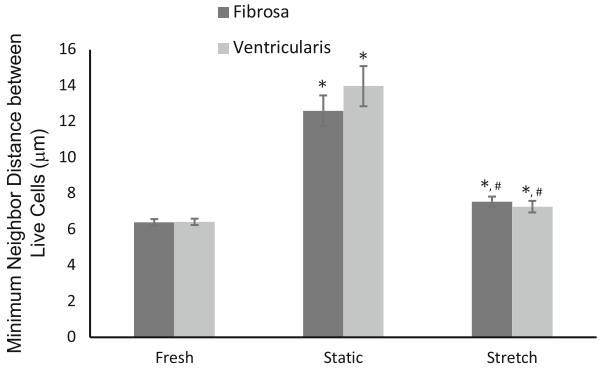

FIGURE 5. Minimum neighbor distance between live cells on the fibrosa and ventricularis surfaces of aortic heart valves. *denotes a significant difference with fresh leaflet samples, #denotes significant difference with static leaflet samples, $p < 0.05$. Error bars represent 95% confidence interval.

stretch device to show endothelial viability and integrity are maintained under normal, physiological conditions where the tissue is stretched 10% in the circumferential direction and 35% in the radial direction.[16] Live cell MND showed a significant increase in distance when valve leaflets were exposed to static culture as compared to fresh or stretched tissue. This indicates that live tissue under static conditions was losing monolayer integrity.

Mechanical Preconditioning

Mechanical preconditioning and stimulation of engineered cardiovascular tissue substitutes is a well-known technique for enhancing tissue formation and organization.[19,24] During the initial stages of TEHV maturation, pulsatile flow enhances cell seeding and alignment within the scaffold.[12] Following seeding, mesenchymal stem cells (MSCs) and fibroblasts increase production of collagen by up to 75% when compared to static cultures.[10,24] This improves mechanical properties of the TEHV with significant increases in ultimate tensile stress and Young's modulus.[10,30] Although collagen synthesis is desirable for *in vitro* maturation of the TEHV, it can lead to mechanically induced valve fibrosis *in vivo*, which can be exacerbated by an inflammatory response that occurs with implantation of a foreign material.[23] Prevention of inflammation can be achieved by the presence of an intact endothelial layer that prevents exposure of the scaffold.[25] The current study examined the response of native heart valve tissue to mechanical preconditioning to understand how autologous ECs would react if seeded onto a TEHV scaffold. The data show that cyclic stretch would be beneficial for maintaining cell viability and preserving endothelial integrity.

Endothelial Integrity

Measurement of the MND showed that leaflets incubated under static conditions started to lose endothelial integrity. Endothelial integrity is related to expression of cell–cell and cell–matrix adhesion proteins, such as VE-cadherin, vinculin and β_1-integrin. VE-Caderin is responsible for cell/cell adhesions and cell motility. More importantly it is responsible for control of intercellular junctions and their integrity and is required to maintain a restrictive endothelial barrier.[32] The state of VE-Cadherin outside the cell is directly proportional to the permeability of the endothelium. Vinculin is a crucial accessory molecule involved in force transduction and mediating cellular response. Vinculin binds integrins to the F-actin network at the intracellular face of the plasma membrane, and subsequently mediates cytoskeletal mechanics.[7] For valvular studies, β_1-integrin behavior is often investigated due to its predominant interaction with collagen.

Previous studies have demonstrated that ventricular ECs increase expression of VE-cadherin and vinculin in response to cyclic strain, whereas fibrosa ECs increase expression of β_1-integrin under elevated strain.[15] Hence, under static conditions there could be a decrease in vinculin and VE-cadherin expression in the ventricularis, which would lead to an increase in the MND and would increase permeability of the endothelial layer.

Study Limitations

This study examined the morphology and viability of ECs on native heart valve tissue in response to cyclic stretch. The experimental system did not incorporate pressure or fluid flow, which are utilized in many current protocols for TEHV *in vitro* maturation. Fluid flow, in particular, is known to influence EC morphology[4,5] and future studies should determine if a synergistic effect exists between cyclic stretch and fluid flow. Other studies that combine mechanical forces have shown favorable results.[10]

CONCLUSION

In conclusion, physiological levels of cyclic stretch maintain endothelial cell viability and integrity when cultured *in vitro* for up to 72 h. These data provide a rationale for incorporating cyclic stretch into the mechanical preconditioning protocols for TEHVs. The presence of an intact endothelium will abate a host inflammatory response that is associated with implantation of a foreign material.

ACKNOWLEDGMENTS

The authors gratefully acknowledge the technical assistance of William Monroe and Amanda Lawrence from the Institute of Imaging and Analytical Technologies at Mississippi State University, and Hemanth Kalluri and Sung Kwang Mun for assistance with MatLab programming.

FUNDING

The National Science Foundation supported these studies through Award 0854153.

CONFLICT OF INTEREST

The authors declare that they have no conflict of interest.

RESEARCH INVOLVING HUMAN AND ANIMAL STUDIES

No human studies were carried out by the authors for this article. No animal studies were carried out by the authors for this article.

REFERENCES

[1]Bach, D. S. Prevalence and characteristics of unoperated patients with severe aortic stenosis. *J. Heart Valve Dis.* 20(3):284–291, 2011.

[2]Benjamin, E. J., S. S. Virani, C. W. Callaway, A. M. Chamberlain, A. R. Chang, S. Cheng, S. E. Chiuve, M. Cushman, F. N. Delling, R. Deo, S. D. de Ferranti, J. F. Ferguson, M. Fornage, C. Gillespie, C. R. Isasi, M. C. Jiménez, L. C. Jordan, S. E. Judd, D. Lackland, J. H. Lichtman, L. Lisabeth, S. Liu, C. T. Longenecker, P. L. Lutsey, J. S. Mackey, D. B. Matchar, K. Matsushita, M. E. Mussolino, K. Nasir, M. O'Flaherty, L. P. Palaniappan, A. Pandey, D. K. Pandey, M. J. Reeves, M. D. Ritchey, C. J. Rodriguez, G. A. Roth, W. D. Rosamond, U. K. A. Sampson, G. M. Satou, S. H. Shah, N. L. Spartano, D. L. Tirschwell, C. W. Tsao, J. H. Voeks, J. Z. Willey, J. T. Wilkins, J. H. Wu, H. M. Alger, S. S. Wong, and P. Muntner. Heart disease and stroke statistics—2018 update: a report from the American Heart Association. *Circulation* 137(12):e67–e492, 2018.

[3]Brody, S., and A. Pandit. Approaches to heart valve tissue engineering scaffold design. *J. Biomed. Mater. Res. Part B* 83(1):16–43, 2007.

[4]Butcher, J. T., A. M. Penrod, A. J. Garcia, and R. M. Nerem. Unique morphology and focal adhesion development of valvular endothelial cells in static and fluid flow environments. *Arterioscler. Thromb. Vasc. Biol.* 24(8):1429–1434, 2004.

[5]Butcher, J. T., C. A. Simmons, and J. N. Warnock. Mechanobiology of the aortic heart valve. *J. Heart Valve Dis*. 17(1):62–73, 2008.
[6]Cawley, P. J., and C. M. Otto. Prevention of calcific aortic valve stenosis-fact or fiction? *Ann. Med.* 41(2):100–108, 2009.
[7]Critchley, D. R. Genetic, biochemical and structural approaches to talin function. *Biochem. Soc. Trans.* 33(Pt 6):1308–1312, 2005.
[8]Danielsen, R., T. Aspelund, T. B. Harris, and V. Gudnason. The prevalence of aortic stenosis in the elderly in Iceland and predictions for the coming decades: the AGES–Reykjavík study. *Int. J. Cardiol.* 176(3):916–922, 2014.
[9]David, T. E. Surgical treatment of aortic valve disease. *Nat. Rev. Cardiol.* 10(7):375, 2013.
[10]Engelmayr, Jr, G. C., V. L. Sales, J. E. Mayer, Jr, and M. S. Sacks. Cyclic flexure and laminar flow synergistically accelerate mesenchymal stem cell-mediated engineered tissue formation: implications for engineered heart valve tissues. *Biomaterials* 27(36):6083–6095, 2006.
[11]Fareed, S. R., A. J. Rajiv, and B. Jagdish. Bioprosthetic heart valves: modes of failure. *Histopathology* 55(2):135–144, 2009.
[12]Flanagan, T. C., C. Cornelissen, S. Koch, B. Tschoeke, J. S. Sachweh, T. Schmitz-Rode, and S. Jockenhoevel. The in vitro development of autologous fibrin-based tissue-engineered heart valves through optimised dynamic conditioning. *Biomaterials* 28(23):3388–3397, 2007.
[13]Head, S. J., M. Celik, and A. P. Kappetein. Mechanical versus bioprosthetic aortic valve replacement. *Eur. Heart J.* 38(28):2183–2191, 2017.
[14]Konduri, S., Y. Xing, J. N. Warnock, Z. He, and A. P. Yoganathan. Normal physiological conditions maintain the biological characteristics of porcine aortic heart valves: an ex vivo organ culture study. *Ann. Biomed. Eng.* 33(9):1158–1166, 2005.
[15]McIntosh, C. T., and J. N. Warnock. Side-specific characterization of aortic valve endothelial cell adhesion molecules under cyclic strain. *J. Heart Valve Dis*. 22(5):631–639, 2013.
[16]Metzler, S. A., C. S. Digesu, J. I. Howard, S. D. Filip To, and J. N. Warnock. Live en face imaging of aortic valve leaflets under mechanical stress. *Biomech. Model. Mechanobiol*. 11(3–4):355–361, 2012.
[17]Metzler, S. A., C. A. Pregonero, J. T. Butcher, S. C. Burgess, and J. N. Warnock. Cyclic strain regulates pro-inflammatory protein expression in porcine aortic valve endothelial cells. *J. Heart Valve Dis*. 17(5):571–577, 2008; (discussion 578).
[18]Mirnajafi, A., B. Zubiate, and M. S. Sacks. Effects of cyclic flexural fatigue on porcine bioprosthetic heart valve heterograft biomaterials. *J. Biomed. Mater. Res. Part A* 94(1):205–213, 2010.
[19]Mol, A., N. J. Driessen, M. C. Rutten, S. P. Hoerstrup, C. V. Bouten, and F. P. Baaijens. Tissue engineering of human heart valve leaflets: a novel bioreactor for a strain-based conditioning approach. *Ann. Biomed. Eng*. 33(12):1778–1788, 2005.
[20]Myles, V., J. Liao, and J. N. Warnock. Cyclic pressure and angiotensin II influence the biomechanical properties of aortic valves. *J. Biomech. Eng*. 136(1):011011, 2014.
[21]Osnabrugge, R. L., D. Mylotte, S. J. Head, N. M. Van Mieghem, V. T. Nkomo, C. M. LeReun, A. J. Bogers, N. Piazza, and A. P. Kappetein. Aortic stenosis in the elderly: disease prevalence and number of candidates for transcatheter aortic valve replacement: a meta-analysis and modeling study. *J. Am. Coll. Cardiol*. 62(11):1002–1012, 2013.
[22]Otsu, N. A threshold selection method from gray-level histograms. *IEEE Trans. Syst. Man Cybernet*. 9:62–66, 1979.
[23]Parvin Nejad, S., M. C. Blaser, J. P. Santerre, C. A. Caldarone, and C. A. Simmons. Biomechanical conditioning of tissue engineered heart valves: too much of a good thing? *Adv. Drug Deliv. Rev*. 96:161–175, 2016.
[24]Ramaswamy, S., D. Gottlieb, G. C. Engelmayr, Jr, E. Aikawa, D. E. Schmidt, D. M. Gaitan-Leon, V. L. Sales, J. E. Mayer, Jr, and M. S. Sacks. The role of organ level conditioning on the promotion of engineered heart valve tissue development in vitro using mesenchymal stem cells. *Biomaterials* 31(6):1114–1125, 2010.
[25]Schmidt, D., P. E. Dijkman, A. Driessen-Mol, R. Stenger, C. Mariani, A. Puolakka, M. Rissanen, T. Deichmann, B. Odermatt, B. Weber, M. Y. Emmert, G. Zund, F. P. Baaijens, and S. P. Hoerstrup. Minimally-invasive implantation of living tissue engineered heart valves: a comprehensive approach from autologous vascular cells to stem cells. *J. Am. Coll. Cardiol*. 56(6):510–520, 2010.
[26]Schoen, F. J., and R. J. Levy. Calcification of tissue heart valve substitutes: progress toward understanding and prevention. *Ann. Thoracic Surg*. 79(3):1072–1080, 2005.
[27]Smith, K. E., S. A. Metzler, and J. N. Warnock. Cyclic strain inhibits acute pro-inflammatory gene expression in aortic valve interstitial cells. *Biomech. Model. Mechanobiol*. 9(1):117–125, 2010.
[28]Soumen, J., and L. Amir. Cells for tissue engineering of cardiac valves. *J. Tissue Eng. Regen. Med*. 10(10):804–824, 2016.
[29]Stewart, B. F., D. Siscovick, B. K. Lind, J. M. Gardin, J. S. Gottdiener, V. E. Smith, D. W. Kitzman, and C. M. Otto. Clinical factors associated with calcific aortic valve disease. *Cardiovasc. Health Study J. Am. Coll. Cardiol*. 29(3):630–634, 1997.
[30]Syedain, Z. H., and R. T. Tranquillo. Controlled cyclic stretch bioreactor for tissue-engineered heart valves. *Biomaterials* 30(25):4078–4084, 2009.
[31]VeDepo, M., E. Buse, R. Quinn, R. Hopkins, and G. Converse. Extended bioreactor conditioning of mononuclear cell-seeded heart valve scaffolds. *J. Tissue Eng*. 9:2041731418767216, 2018.
[32]Vestweber, D. VE-cadherin: the major endothelial adhesion molecule controlling cellular junctions and blood vessel formation. *Arterioscler. Thromb. Vasc. Biol*. 28(2):223–232, 2008.
[33]Warnock, J. N., C. A. Gamez, S. A. Metzler, J. Chen, S. H. Elder, and J. Liao. Vasoactive agents alter the biomechanical properties of aortic heart valve leaflets in a time-dependent manner. *J. Heart Valve Dis*. 19(1):86–95, 2010; (discussion 96).
[34]Xing, Y., Z. He, J. N. Warnock, S. L. Hilbert, and A. P. Yoganathan. Effects of constant static pressure on the biological properties of porcine aortic valve leaflets. *Ann. Biomed. Eng*. 32(4):555–562, 2004.
[35]Xing, Y., J. N. Warnock, Z. He, S. L. Hilbert, and A. P. Yoganathan. Cyclic pressure affects the biological properties of porcine aortic valve leaflets in a magnitude and frequency dependent manner. *Ann. Biomed. Eng*. 32(11):1461–1470, 2004.

[36]Yap, C. H., H. S. Kim, K. Balachandran, M. Weiler, R. Haj-Ali, and A. P. Yoganathan. Dynamic deformation characteristics of porcine aortic valve leaflet under normal and hypertensive conditions. *Am. J. Physiol. Heart Circ. Physiol.* 298(2):H395–H405, 2010.